Available online at www.sciencedirect.com

SCIENCE DIRECT®

Physics Letters B 633 (2006) 61–69

PHYSICS LETTERS B

www.elsevier.com/locate/physletb

Comment on form-factor shape and extraction of $|V_{ub}|$ from $B \to \pi l \nu$

Thomas Becher [a], Richard J. Hill [b,*]

[a] *Fermi National Accelerator Laboratory, PO Box 500, Batavia, IL 60510, USA*
[b] *Stanford Linear Accelerator Center, Stanford University, Stanford, CA 94309, USA*

Received 13 September 2005; received in revised form 4 November 2005; accepted 19 November 2005

Available online 1 December 2005

Editor: H. Georgi

Abstract

We point out that current experimental data for partial $B \to \pi l \nu$ branching fractions reduce the theoretical input required for a precise extraction of $|V_{ub}|$ to the form-factor normalization at a single value of the pion energy. We show that the heavy-quark expansion provides a bound on the form-factor shape that is orders of magnitude more stringent than conventional unitarity bounds. We find $|V_{ub}| = (3.7 \pm 0.2 \pm 0.1) \times [0.8/F_+(16\ \text{GeV}^2)]$. The first error is from the experimental branching fractions, and the second is a conservative bound on the residual form-factor shape uncertainty, both of which will improve with additional data. Together with current and future lattice determinations of the form-factor normalization this result gives an accurate, model independent determination of $|V_{ub}|$. We further extract semileptonic shape observables such as $|V_{ub} F_+(0)| = 0.92 \pm 0.11 \pm 0.03$ and show how these observables can be used to test factorization and to determine low-energy parameters in hadronic B decays.

1. Introduction

Measuring the magnitude of the weak mixing matrix element V_{ub} is important for constraining the unitarity triangle and testing the standard model of weak interactions. The exclusive determination of $|V_{ub}|$ requires knowledge of the relevant heavy-to-light meson form factor and in the past this has led to significant model dependence in the result. First, the methods that were used to calculate the form factor, such as light-cone sum rules, quark models and quenched lattice calculations, all have unknown systematic errors. Second, each of these methods covers only part of the kinematic range; to obtain the total decay rate, the results were extrapolated using simplified parameterizations for the momentum dependence of the form factor. In the past year, the situation has improved dramatically: there are now several measurements of partial $B \to \pi l \nu$ branching fractions [1–4] and the first results for the form factor from precision lattice simulations with dynamical light quarks have been presented [5,6]. We show in this Letter that if theoretical bounds on the form factor are taken into account, the experimental results for the partial branching fractions determine the shape of the form factor, to the point where no shape information at all is required from theory. This reduces the theoretical input for the determination of $|V_{ub}|$ to a normalization of the relevant form factor, which can be taken at an energy within the range studied with current lattice simulations. For the first time, this allows an accurate, model independent, determination of $|V_{ub}|$ from exclusive semileptonic decays.

Bounds on the form factor can be derived via the computation of an appropriately chosen correlation function in perturbative QCD. By unitarity and analyticity, the resulting "dispersive bound" constrains the behavior of the form factor in the semileptonic region [7–10], and may be expressed as a condition on the coefficients in a convergent series expansion. While these bounded "series parameterizations" have been around for more than twenty-five years, many papers on the subject (in particular all experimental papers) have instead used simple pole forms to parameterize the form factor. In order to unify these descriptions, and to explain the dispersive bounds in a simple setting, we compare the class of series parameterizations emerging from the conventional dispersive bound analysis to the class of "pole parameterizations" introduced in [11,12]. Both repre-

* Corresponding author.
E-mail address: rjh@slac.stanford.edu (R.J. Hill).

0370-2693
doi:10.1016/j.physletb.2005.11.063

sentations are exact, in the sense that the true form factor is guaranteed to be described arbitrarily well by a member of the class, and dispersive bounds can be established for both classes by power counting in the heavy-quark mass. With the resulting constraints in place, stable fits without truncation to a fixed number of parameters can be performed. In fact, for the series parameterization, we show that the bound given by simple heavy-quark power counting is orders of magnitude more stringent than the bound based on unitarity, thus providing much better control over the extraction of physical observables from the data. We also derive three new exact sum rules for the coefficients appearing in the series representation of the form factor.

The Letter is organized as follows. In Section 2 we review the pole and series parameterizations of the form factor. We list the experimental and lattice data to be used throughout the Letter, and for later comparison we determine $|V_{ub}|$ using three-parameter truncations of these parameterizations. Section 3 then introduces the bounds associated with each parameterization, and establishes conservative estimates based on heavy-quark power counting for the bounded quantities. Section 4 examines the maximal precision for $|V_{ub}|$ that can be reached with present data. We show that with a form-factor determination at intermediate q^2 values, within the range studied in current lattice simulations, the experimental uncertainty on $|V_{ub}|$ is well below 10%, whereas a form-factor determination near maximal q^2 would not translate into a precise value of $|V_{ub}|$. We introduce three shape observables, $|V_{ub}F_+(0)|$, $F'_+(0)/F_+(0)$ and α, and discuss their sensitivity to the exact value of the bound. In Section 5, having established our procedure, we present final values for $|V_{ub}|$, and for $F_+(0)$, in terms of a single lattice data point, $F_+(16\ \mathrm{GeV}^2)$. We extract the shape observables, which are determined by the experimental semileptonic data alone, and show how these observables provide important constraints on the factorization approach to hadronic B decays.

2. Form-factor parameterizations and extraction of $|V_{ub}|$

Having restricted the shape of the q^2 spectrum, or equivalently, of the form factor, by experimental measurements, the central value and errors for $|V_{ub}|$ are determined by varying the allowed form factor over all "reasonable" curves that are consistent with the data, and with a normalization of the form factor taken from theory at a given value (or multiple values) of q^2. Defining this procedure precisely requires specifying a class of curves that contains the true form factor (to a precision compatible with the data), and that is sufficiently rich to describe all variations impacting the observables under study. A statistical analysis along standard lines then determines central values and errors for the desired observable quantities.

A starting point to isolate such a class of curves is the dispersive representation of the relevant form factor:

$$F_+\big(q^2\big) = \frac{F_+(0)/(1-\alpha)}{1-\frac{q^2}{m_{B^*}^2}} + \frac{1}{\pi}\int\limits_{t_+}^{\infty} dt\, \frac{\operatorname{Im} F_+(t)}{t-q^2-i\epsilon}. \tag{1}$$

Here α is defined by the relative size of the contribution to $F_+(0)$ from the B^* pole, and $t_\pm \equiv (m_B \pm m_\pi)^2$. For massless leptons, the semileptonic region is given by $0 \leqslant q^2 \leqslant t_-$. Eq. (1) states that, after removing the contribution of the B^* pole lying below threshold, $F_+(q^2)$ is analytic outside of a cut in the complex q^2-plane extending along the real axis from t_+ to ∞, corresponding to the production region for states with the appropriate quantum numbers.

One class of parameterizations keeps the B^* pole explicit and approximates the remaining dispersion integral in (1) by a number of effective poles:

$$F_+\big(q^2\big) = \frac{F_+(0)/(1-\alpha)}{1-\frac{q^2}{m_{B^*}^2}} + \sum_{k=1}^{N} \frac{\rho_k}{1-\frac{1}{\gamma_k}\frac{q^2}{m_{B^*}^2}}. \tag{2}$$

The true form factor can be approximated to any desired accuracy by introducing arbitrarily many, finely-spaced, effective poles. In the next section, we derive a bound on the magnitudes, $|\rho_k|$, of the coefficients of the effective poles. This allows a meaningful $N \to \infty$ limit, thus enabling us to investigate the behavior of the fits when arbitrarily many parameters are included. We find in actuality that current data cannot yet resolve more than one distinct effective pole in addition to the B^* pole. Parameterizations of the above type are widely used to fit form factors. In particular, a simplified version of the $N = 1$ case, the so-called Becirevic–Kaidalov (BK) parameterization [11] is used in many recent lattice calculations and experimental studies. As shown in [12], this two-parameter form is overly restrictive since it enforces scaling relations which at small q^2 are broken by hard gluon exchange. The size of these hard-scattering terms, which appear at leading order in the heavy-quark expansion, is subject to some controversy and constraining their size is an important task. The parameterization of the form factors should allow for their presence.

Another class of parameterizations is obtained by expanding the form factor in a series around some $q^2 = t_0$ in the semileptonic region up to a fixed order, with the coefficients of this expansion as the fit parameters. The convergence of this simple expansion is very poor due to the presence of the nearby singularities at $q^2 = m_{B^*}^2$ and $q^2 = t_+$. However, an improved series expansion of the form factor that converges in the entire cut q^2-plane is obtained after a change of variables that maps this region onto the unit disc $|z| < 1$. In terms of the new variable, F_+ has an expansion

$$F_+\big(q^2\big) = \frac{1}{P(q^2)\phi(q^2,t_0)} \sum_{k=0}^{\infty} a_k(t_0)\big[z\big(q^2,t_0\big)\big]^k,$$
$$z\big(q^2,t_0\big) = \frac{\sqrt{t_+-q^2}-\sqrt{t_+-t_0}}{\sqrt{t_+-q^2}+\sqrt{t_+-t_0}}, \tag{3}$$

with real coefficients a_k. The variable $z(q^2,t_0)$ maps the interval $-\infty < q^2 < t_+$ onto the line segment $-1 < z < 1$, with the free parameter $t_0 \in (-\infty, t_+)$ corresponding to the value of q^2 mapping onto $z = 0$. Points immediately above (below) the q^2-cut are mapped onto the lower (upper) half-circle $|z| = 1$. The function $P(q^2) \equiv z(q^2, m_{B^*}^2)$ accounts for the pole in $F_+(q^2)$

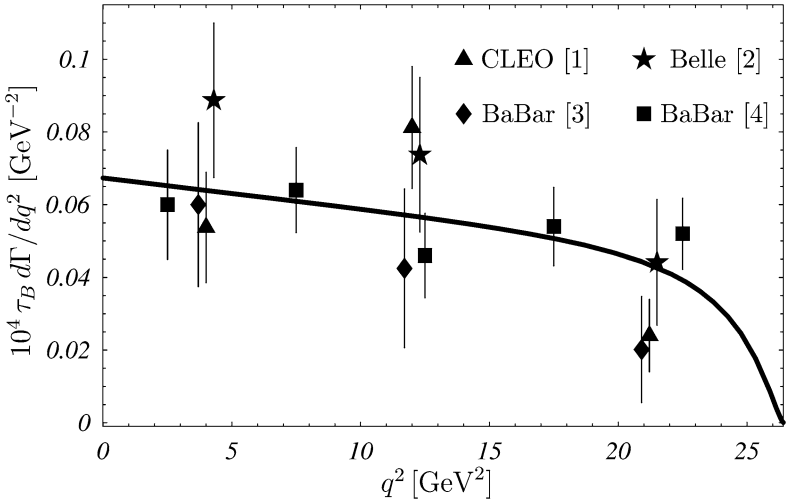

Fig. 1. Experimental data for the partial $\bar{B}^0 \to \pi^+\ell^-\bar{\nu}$ branching ratios and fit result shown as solid line. The fit results from (2) with $N = 1$ and (5) with $k_{\max} = 2$ are indistinguishable. Note that the experimental data is binned: [1–3] give the result in three bins, while [4] gives the result in five q^2-bins. We plot the value and error divided by the bin width at the average q^2-value in each bin. For the three-bin results, we have slightly shifted the points to the left and right to increase visibility.

at $q^2 = m_{B^*}^2$, while $\phi(q^2)$ is any function analytic outside of the cut. It is interesting to note that this reorganization succeeds in turning a large recoil parameter, $(v\cdot v')_{\max} - 1 \approx 18$, into a small expansion parameter. For example, for $t_0 = 0$ the variable z is negative throughout the semileptonic region and

$$|z|_{\max} = \frac{\sqrt{(v\cdot v')_{\max}+1}-\sqrt{2}}{\sqrt{(v\cdot v')_{\max}+1}+\sqrt{2}} \approx 0.5, \tag{4}$$

where v and v' are the velocities of the B and π mesons. The same size, but for positive z is obtained for $t_0 = t_-$. By choosing the intermediate value $t_0 = t_+(1-\sqrt{1-t_-/t_+})$, the expansion parameter can be made as small as $|z|_{\max} \approx 0.3$. A second class of parameterizations is obtained by a truncation of the above series:

$$F_+\big(q^2\big) = \frac{1}{P(q^2)\phi(q^2,t_0)} \sum_{k=0}^{k_{\max}} a_k(t_0)\big[z\big(q^2,t_0\big)\big]^k. \tag{5}$$

As discussed in the next section, it is conventional to take

$$\phi\big(q^2,t_0\big) = \left(\frac{\pi m_b^2}{3}\right)^{1/2}\left(\frac{z(q^2,0)}{-q^2}\right)^{5/2}\left(\frac{z(q^2,t_0)}{t_0-q^2}\right)^{-1/2} \times \left(\frac{z(q^2,t_-)}{t_--q^2}\right)^{-3/4}\frac{(t_+-q^2)}{(t_+-t_0)^{1/4}}. \tag{6}$$

With this choice, a bound $\sum_k a_k^2 \lesssim 1$ is obtained by perturbative methods.[1] Together with the restriction $|z| < 1$, this allows a meaningful $k_{\max} \to \infty$ limit. In actuality, we find that current data can only resolve the first three terms in the series (5).

Fig. 1 shows the available experimental data on the partial branching fraction $d\Gamma(\bar{B}^0 \to \pi^+\ell^-\bar{\nu})/dq^2$. The CLEO [1], Belle [2] and BaBar [4] Collaborations have measured this branching fraction in three separate q^2-bins and BaBar [3] has presented a measurement using five q^2-bins. The correlation matrix is included in our fits for the data in [1]. For the remaining data, q^2-bins are taken as uncorrelated. In order to extract $|V_{ub}|$ we also need the normalization of the form factor. The $B \to \pi$ vector form factors have recently been determined by the Fermilab Lattice [5] and by the HPQCD [6] Collaborations in lattice simulations with dynamical fermions. The preliminary results of these calculations give $F_+(16\ \mathrm{GeV}^2) = 0.81 \pm 0.11$ [5] and $F_+(16\ \mathrm{GeV}^2) = 0.73 \pm 0.10$ [6].[2] Although the lattice calculations give the form factor at several different q^2-values, the correlations between different points are not available and it is difficult to quantify the uncertainty on the shape. Anticipating the analysis of Section 4, where we determine the range of q^2 that best exploits the experimental shape information, we use $F_+(16\ \mathrm{GeV}^2) = 0.8 \pm 0.1$ as our default value for the form-factor normalization. Note that we have avoided any theoretical biases concerning the form-factor shape. Performing a χ^2 fit yields $|V_{ub}| = 3.7^{+0.6}_{-0.5} \times 10^{-3}$ for both the parameterization (2) with $N = 1$, and (5) with $k_{\max} = 2$.

Fig. 2 shows the 68% and 95% confidence limits for $|V_{ub}|$ as a function of the value and uncertainty of the form factor at $q^2 = 16\ \mathrm{GeV}^2$. The form-factor normalization is the dominant error in the determination of $|V_{ub}|$; if the quantity $F_+(16\ \mathrm{GeV}^2)$ would be known exactly, the uncertainty on $|V_{ub}|$ would drop to approximately 6%. The quality of the fit is equally good for

[1] For different t_0, the expansion parameters, $z \equiv z(t,t_0)$ and $z' \equiv z(t,t_0')$, and expansion coefficients, $a_k \equiv a_k(t_0)$ and $a_k' \equiv a_k(t_0')$, are related by the Möbius transformation:

$$z' = \frac{z(t_0,t_0')+z}{1+z(t_0,t_0')z}, \qquad \sqrt{1-z^2}\sum_{k=0}^{\infty} a_k z^k = \sqrt{1-z'^2}\sum_{k=0}^{\infty} a_k' z'^k.$$

It is easily verified that the sum of squares of coefficients is invariant under such a transformation, $\sum_k a_k^2 = \sum_k a_k'^2$, as guaranteed by the construction of ϕ, see (9).

[2] The parameterization (2) with $N = 1$ has been used to interpolate to the common q^2-point, and for definiteness the errors are taken as those from the nearest points: $q^2 = 15.87\ \mathrm{GeV}^2$ [5], with statistical and systematic errors added in quadrature, and $q^2 = 16.28\ \mathrm{GeV}^2$ [6].

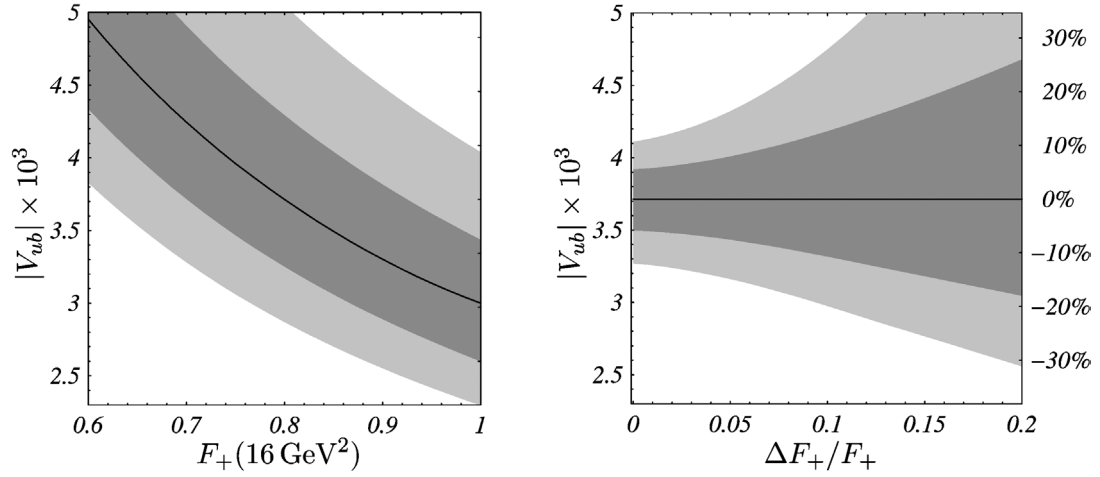

Fig. 2. 68% (dark) and 95% (light) confidence limits for $|V_{ub}|$ determined by fitting the parameterizations (2) or (5) to experimental data in [1–4], with the single lattice data point $F_+(16\ \mathrm{GeV}^2) = 0.8 \pm 0.1$. Results from (2) and (5) are indistinguishable. The plot on the right shows $|V_{ub}|$ for fixed $F_+(16\ \mathrm{GeV}^2) = 0.8$ as a function of the relative uncertainty on the form factor.

both parameterizations, with $\chi^2 = 12.0$.[3] The extracted value of $|V_{ub}|$ is insensitive to the choice of the free parameter t_0. Setting $\phi(q^2) = 1$ in (5) also has negligible impact, and similarly adding more lattice input points does not substantially change the result if the dominant lattice errors are correlated. The effect of allowing additional terms in the parameterizations (2) and (5) is investigated in the following sections. We will find that the result for the value and uncertainty of $|V_{ub}|$ from the simple parameterizations used in this section is not appreciably altered if additional terms are included.

3. Form-factor bounds

To make a fully rigorous determination of $|V_{ub}|$, the truncation to the three-parameter classes of curves considered in the previous section requires justification. For instance, if the neglected terms in (2) or (5) conspired to produce a sharp peak in the form factor at precisely the value of the lattice input point, then the integrated rate would be overestimated, and the value of $|V_{ub}|$ underestimated. To prevent this from happening requires some bound on the perversity of allowed form-factor shapes. In practice, we would like to ensure that our extraction of physical observables is "model-independent" by allowing for arbitrarily many parameters, i.e., taking $N \to \infty$ in (2) and $k_{\max} \to \infty$ in (5). Retaining predictive power then demands that a bound be enforced on the parameters appearing in these expansions.

To bound the coefficients ρ_k in the expansion (2), we introduce a decomposition of the integration region, $t_+ \leqslant t_1 < \cdots < t_{N+1} < \infty$, and define

$$\rho_k \equiv \frac{1}{\pi} \int_{t_k}^{t_{k+1}} \frac{dt}{t} \operatorname{Im} F_+(t), \qquad \gamma_k \equiv \frac{t_k}{m_{B^*}^2}. \tag{7}$$

Since $F_+(t) \sim t^{-1}$ at large t, it follows that

$$\sum_k |\rho_k| \leqslant \frac{1}{\pi} \int_{t_+}^{\infty} \frac{dt}{t} \big|F_+(t)\big| \equiv R, \tag{8}$$

and this is the desired bound. The integral in (8) is dominated by states with $t - t_+ \sim m_b \Lambda$, where $F_+ \sim m_b^{1/2}$, so that the quantity R is parametrically of order $(\Lambda/m_b)^{1/2}$, with Λ a hadronic scale. To be sure that the bound deserves the model-independent moniker, one should use a very conservative estimate. In our fits we will use $R \leqslant \sqrt{10}$ and $R \leqslant 10$, i.e., we allow for an addition factor of 100 or 1000 beyond the dimensional estimate $R^2 \sim \Lambda/m_b \sim 0.1$.

The coefficients a_k in the expansion (5) can be bounded by requiring that the production rate of $B\pi$ states, described by the analytically continued form factor, does not overwhelm the production rate of *all* states coupling to the current of interest (in this case, the vector current $\bar{u}\gamma^\mu b$). The latter rate is computable in perturbative QCD using the operator product expansion (for a pedagogical discussion, see, e.g., [10]). The function ϕ in (6) was chosen such that the fractional contribution of $B\pi$ states to this rate is given at leading order by

$$\sum_{k=0}^{\infty} a_k^2 = \frac{1}{2\pi i} \oint \frac{dz}{z} \big|\phi(z) P(z) F_+(z)\big|^2 = \frac{m_b^2}{3} \int_{t_+}^{\infty} \frac{dt}{t^5} \big[(t - t_+)(t - t_-)\big]^{3/2} \big|F_+(t)\big|^2 \equiv A. \tag{9}$$

In the heavy-quark limit, the leading contributions to the integral A in (9) are of order $(\Lambda/m_b)^3$ and arise from two regions: the region close to threshold, $t - t_+ \sim m_b \Lambda$, where the pion has

[3] Note that all three-bin measurements determine the same observable quantities. The minimal χ^2 obtained from the three-bin measurements is 5.0 for 9–3 degrees of freedom. This value measures the (good) agreement between the three-bin measurements, and should be subtracted from the total in order to obtain a measure of agreement between the data and the parameterizations. The resulting quality of our fit is good: 12.0–5.0 for 9–4 degrees of freedom.

energy $E \sim \Lambda$ and the form factor scales as $F_+ \sim m_b^{1/2}$; and the region $t - t_+ \sim m_b^2$, where $E \sim m_b$ and $F_+ \sim m_b^{-3/2}$ (for a discussion of the form-factor scalings, see [12]). The region of very high energies $t \gg m_b^2$, where $F_+ \sim 1/t$, gives a subleading contribution.

Since, by definition, the fraction is smaller than unity, it is conventional to take the loose bound $A \leqslant 1$, which does not make use of scaling behavior in the heavy-quark limit. Clearly this bound leaves much room for improvement; from its scaling behavior, we expect A to be on the order of a few permille. This implies that higher-order perturbative and power corrections in the operator product analysis introduce negligible error, as noticed in [13]. It is also easy to see that the dispersive bounds by themselves do not impose tight constraints on the form-factor shape. Since the scale of the coefficients is set by $a_0 \sim m_b^{-3/2}$, even with the optimal choice $|z|_{\max} \approx 0.3$, the dispersive bounds allow the relative size of higher-order terms in the series, $|a_k z^k/a_0|$, to be of order unity up to $k \approx 4$, and to contribute significantly for even higher k. This situation for heavy-to-light decays such as $B \to \pi$ contrasts with that for heavy–heavy decays such as $B \to D$ [14,15], where the bound is parametrically of order unity (counting $m_c \sim m_b \gg \Lambda$). For this case, the scale of the coefficients is set by $a_0 \sim m_b^0$, and with $|z|_{\max} \approx 0.06$ the bound ensures that only the first few terms in the series are required for percent accuracy.

To put the dispersive bounds in perspective, it may be useful to emphasize that establishing an order-of-magnitude bound on any integral of the form $\int_{t_+}^{\infty} dt\, k(t)|F_+(t)|^2$ for some $k(t)$ would yield an equally valid, bounded, parameterization, with a new $\phi(t)$ constructed from $k(t)$ as in (6) and (9). Similarly, bounded pole parameterizations (2) are obtained by establishing an order-of-magnitude bound on any integral of the form $\int_{t_+}^{\infty} dt\, k(t)|F_+(t)|$ for some $k(t)$, as in (7) and (8). Focusing attention on the special case of (6) and (9) is justified only to the extent that the bound (9) is sufficiently restrictive, and to the extent that similar or tighter bounds cannot be conservatively estimated by other means.

It is interesting to note that the two bounds are not equivalent. The bound $\sum_k |\rho_k| \leqslant R < \infty$ uses the fact that the asymptotic form factor can be evaluated in perturbation theory, where the scaling $F_+(t) \sim t^{-1}$ is found at large t. This condition is not automatically satisfied by the series parameterization (5), which as seen from (9) requires only $F_+(t) \lesssim t^{1/2}$ at large t. Imposing the proper large-t behavior yields the sum rules

$$\frac{d^n}{dz^n} P(z)\phi(z)F(z)\bigg|_{z=1} = 0 \quad \leftrightarrow \quad \sum_{k=0}^{\infty} k^n a_k z^k\bigg|_{z\to 1} = 0, \qquad n = 0, 1, 2. \tag{10}$$

To our knowledge, the above sum rules have not been discussed in the literature. On the other hand, all pole parameterizations "violate" the bound $\sum_{k=0}^{\infty} a_k^2 \equiv A < \infty$ for the simple reason that the integral in (9) is not well defined for these parameterizations, because $F_+(t)$ has poles on the integration contour.

The bounds discussed here are associated with the behavior of the form factor above threshold. Since we are interested in the form factor in the semileptonic region, these higher-energy properties are useful only to the extent that they can help to constrain the form factor in this region. Incorrect high-energy behavior therefore does not imply that a given parameterization cannot be used to describe low-energy data. For instance, the effective poles in (2) could be smeared into finite-width effective resonances in order to make the integral in (9) converge; however, the semileptonic data is very insensitive to such fine-grained detail, and this modification has a very minor impact on the fits. Similarly, unless the bound (9) is close to being saturated, the coefficients a_k for moderately large k in the series parameterization (5) can be tuned to satisfy the sum rules (10), or equivalently, to make the integral in (8) converge. However, the semileptonic data becomes insensitive to terms z^k for large k, and again such a modification has little impact on the fits. Thus, while at some level the bound (8) will constrain the parameters in the series parameterization (5), and the bound (9) will constrain the parameters in the pole parameterization (2), we restrict attention to the constraints imposed by (8) on the pole parameterization, and by (9) on the series parameterization.

4. Parameterization uncertainty and shape observables

With the bounds in place, it is straightforward to generalize the fits in Section 2 to include arbitrarily many parameters. Imposing the very conservative bound $\sum_k |\rho_k| < 10$, we observe that additional poles in the class of parameterizations (2) have essentially no impact on the central value and errors for $|V_{ub}|$. Similarly, using the very conservative bound $\sum_k a_k^2 < 1$ in (5), we find that the inclusion of higher-order terms beyond $k_{\max} = 2$ has negligible impact on $|V_{ub}|$. The errors are dominated by the lattice input point, and both the central value and errors are not changed significantly from the $N = 1$ or $k_{\max} = 2$ fits in Section 2.

In order to isolate the uncertainty on the form-factor shape inherent to the present data, we show in Fig. 3 the minimum attainable error on $|V_{ub}|$, assuming exact knowledge of the form factor at one q^2-value. Results are shown for the parameterization (5), using various bounds $\sum_k a_k^2 < 0.01$, 0.1 and 1. As the figure illustrates, points in the intermediate range of q^2 lead to the smallest uncertainty on $|V_{ub}|$, and for these points, the $|V_{ub}|$ extraction is not very sensitive to even the order of magnitude of the chosen bound, with the minimum error varying from approximately 6% to approximately 8% as the bound is relaxed from 0.01 to 1. It should be noted that a better understanding of correlations in the experimental data would be necessary when probing this level of precision. The curves in Fig. 3 are also indicative of the impact of additional theory inputs. Performing the fits with data points at different q^2-values in addition to the default $F_+(16\ \text{GeV}^2)$ shows that a point at $q^2 = 0$ would require $\lesssim 10\%$ error to significantly decrease the error on $|V_{ub}|$, while even exact knowledge of the form factor at $q^2 = t_-$ has almost no impact.

In the remainder of this section we consider observables which are more sensitive to the shape of the form factor and investigate the role played by the bounds in these cases. In particular, we extract the form factor and its first derivative at

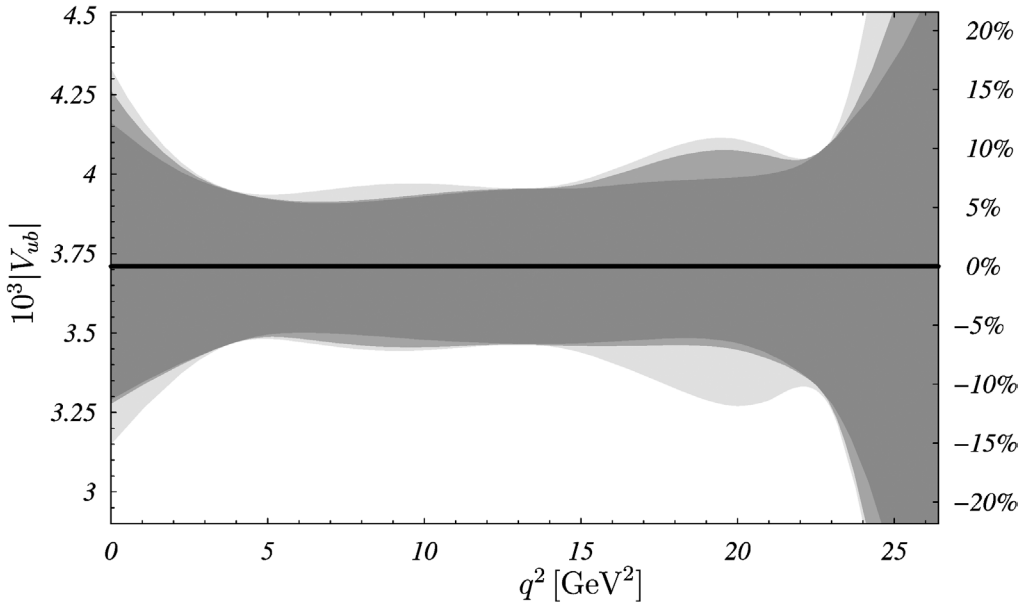

Fig. 3. $\Delta\chi^2 = 1$ region for $|V_{ub}|$ for an infinitely precise form-factor determination at a single q^2-value. The plot assumes that the form factor yields the central value $|V_{ub}| = 3.7 \times 10^{-3}$. The darkest band is obtained for $\sum_k a_k^2 < 0.01$, while the two lighter bands correspond to $\sum_k a_k^2 < 0.1$ and $\sum_k a_k^2 < 1$.

$q^2 = 0$, as well as the residue at the B^* pole, which is directly related to the parameter α, as in (1). These quantities are interesting in their own right. The form factor at zero momentum transfer, normalized as $|V_{ub}|F_+(0)$, is an important input for the evaluation of factorization theorems for charmless two-body decays such as $B \to \pi\pi$. The derivative of the form factor at $q^2 = 0$, conveniently normalized as $(m_B^2 - m_\pi^2)F'_+(0)/F_+(0)$, determines the quantity δ measuring the ratio of hard-scattering to soft-overlap terms in the form factor [12]. Finally, the value of $(1-\alpha)^{-1}$ is proportional to the coupling constant $g_{B^*B\pi}$. The observable quantities $|V_{ub}|F_+(0)$, $F'_+(0)/F_+(0)$ and α are independent of the form-factor normalization, and hence are determined solely by the experimental data.

In Tables 1 and 2, we show how the results for the shape observables change when additional parameters are included. For the pole parameterization (2) we perform fits with $N = 1$, 2 and 3 poles in addition to the B^* pole. (The case $N = 1$ was studied in [12].) To help stabilize the fits, we impose a minimum spacing of the poles $\gamma_{k+1} - \gamma_k > 1/N$, and a maximum pole position, $\gamma_k < N + 1$. For the polynomial parameterization (5), we set $k_{\max} = 2$, 3 and 4. We perform each of the fits with two different bounds—a very loose model-independent bound, and a more stringent bound that relies on the scaling behavior of the bounded quantity in the heavy-quark limit. Given a value of the bound, a central value and errors are determined by taking the limit of large N in (2), or large $k_{\max}$ in (5). The sequence converges once the size of the neglected terms is constrained by the bound to lie below the sensitivity of the chosen observable.

The quantities $|V_{ub}|F_+(0)$, $F'_+(0)/F_+(0)$ and α exhibit different sensitivities to the bounds. This is to be expected, since sharp bends in the fitted curve at the endpoints allowed by the additional terms can have strong effects on the slope, or on the residue of the B^* pole, but are not constrained tightly by the data. Imposing only very loose bounds therefore leads to large uncertainties for these quantities.

It is instructive to examine the relation between observables and expansion coefficients. At $t_0 = 0$ the quantities $f(0)$, α, β and δ studied in [12] are related to the coefficients a_k by

$$f(0) \equiv F_+(0) = \frac{16 a_0}{\hat m_b}\left(\frac{3}{\pi}\right)^{1/2} \frac{(1+\hat m_\pi)^{5/2}}{(1+\sqrt{\hat m_\pi})^3} \frac{1+\hat m_\pi + \hat\Delta}{1+\hat m_\pi - \hat\Delta},$$

$$\begin{aligned} 1+\beta^{-1}-\delta &\equiv \frac{m_B^2 - m_\pi^2}{F_+(0)} \frac{dF_+}{dq^2}\bigg|_{q^2=0} \\ &= \frac{-a_1}{4a_0}\frac{1-\hat m_\pi}{1+\hat m_\pi} + \frac{3}{4}\frac{1-\sqrt{\hat m_\pi}}{1+\sqrt{\hat m_\pi}} + \frac{\hat\Delta(1-\hat m_\pi)}{(1+\hat m_\pi)^2 - \hat\Delta^2}, \\ (1-\alpha)^{-1} &= \frac{(1+\hat m_\pi+\hat\Delta)^2(1+\sqrt{\hat m_\pi})^3}{4(1+\hat m_\pi)^2(\hat\Delta + 2\sqrt{\hat m_\pi})^{3/2}} \\ &\quad \times \sum_{k=0}^{\infty} \frac{a_k}{a_0}\left((-1)\frac{1+\hat m_\pi - \hat\Delta}{1+\hat m_\pi+\hat\Delta}\right)^k, \end{aligned} \tag{11}$$

where $\Delta^2 \equiv (m_B + m_\pi)^2 - m_{B^*}^2$, and hats denote quantities in units of m_B. The heavy-quark scaling laws for $f(0)$ and $1+\beta^{-1}-\delta$ are special cases of the general law $a_k \sim m_b^{-3/2}$, obtained by taking k derivatives in (3), and noticing that $d^n F_+/d(\hat q^2)^n|_{q^2=0} \sim m_b^{-3/2}$ when scaling violations are neglected. Similarly, the scaling law for $(1-\alpha)^{-1}$ translates into the behavior $\hat\Delta^{-1/2} \sim m_b^{1/4}$ for the sum appearing in the last equation of (11).

5. Results and discussion

In order to extract the most precise value of $|V_{ub}|$, it is important to make full use of the existing experimental data for $B \to \pi l \nu$ that determines the form-factor shape. To emphasize this point, the analysis was done here using no shape information at all from theory, but only a normalization at one

Table 1
Fit results for form-factor shape parameters using the pole parameterization (2)

Bound	$\sum_k \lvert\rho_k\rvert = 10$			$\sum_k \lvert\rho_k\rvert = \sqrt{10}$		
N	1	2	3	1	2	3
$\sum_k \lvert\rho_k\rvert$	1.02	1.36	10	1.02	1.36	$\sqrt{10}$
χ^2	11.97	11.96	11.58	11.97	11.96	11.80
$10^3\lvert V_{ub}\rvert F_+(0)$	$0.93^{+0.06}_{-0.09}$	$0.93^{+0.11}_{-0.09}$	$0.87^{+0.14}_{-0.12}$	$0.93^{+0.06}_{-0.09}$	$0.93^{+0.10}_{-0.09}$	$0.91^{+0.11}_{-0.10}$
$\frac{(m_B^2-m_\pi^2)F'_+(0)}{F_+(0)}$	$1.3^{+0.4}_{-0.1}$	$1.3^{+0.4}_{-0.7}$	$2.0^{+0.9}_{-1.2}$	$1.3^{+0.4}_{-0.1}$	$1.3^{+0.4}_{-0.6}$	$1.5^{+0.6}_{-0.8}$
$(1-\alpha)^{-1}$	5^{+5}_{-3}	6^{+6}_{-5}	6^{+20}_{-15}	5^{+5}_{-3}	6^{+6}_{-5}	6^{+6}_{-8}

Table 2
Fit results for form-factor shape parameters using the series parameterization (5) with $t_0 = 0$

Bound	$\sum_k a_k^2 < 1$			$\sum_k a_k^2 < 0.01$		
$k_{\max}$	2	3	4	2	3	4
$\sum_k a_k^2$	0.003	0.3	1	0.003	0.01	0.01
χ^2	12.0	11.7	11.7	12.0	11.9	11.9
$10^3\lvert V_{ub}\rvert F_+(0)$	$0.93^{+0.10}_{-0.10}$	$0.87^{+0.15}_{-0.15}$	$0.87^{+0.14}_{-0.14}$	$0.93^{+0.10}_{-0.10}$	$0.92^{+0.11}_{-0.10}$	$0.92^{+0.11}_{-0.10}$
$\frac{(m_B^2-m_\pi^2)F'_+(0)}{F_+(0)}$	$1.3^{+0.6}_{-0.5}$	$2.0^{+1.4}_{-1.4}$	$2.0^{+1.4}_{-1.4}$	$1.3^{+0.6}_{-0.4}$	$1.4^{+0.6}_{-0.6}$	$1.5^{+0.6}_{-0.6}$
$(1-\alpha)^{-1}$	6^{+2}_{-2}	13^{+8}_{-14}	9^{+20}_{-17}	6^{+2}_{-2}	7^{+2}_{-5}	8^{+2}_{-6}

q^2-point. Our results make it clear that the limiting factor in the determination of $|V_{ub}|$ is currently the form-factor normalization, with very small uncertainty associated with the form-factor shape. Similar conclusions are implicit in other recent works. For example, in [13] the reduction in error compared to methods employing only total experimental branching fractions is due almost entirely to the inclusion of shape information from experiment, and not to the inclusion of additional theory input points. In [16], experimental data is combined with simple parameterizations of the form-factor shape to constrain the hadronic input parameters appearing in sum rule estimates of the form factor. In contrast to these and other previous works, we have avoided any theoretical biases concerning the form-factor shape.

In practical terms, the parameterizations (2), with $N = 1$, and (5), with $k_{\max} = 2$, are sufficient for describing the current generation of semileptonic data, in the sense that the addition of more parameters does not significantly improve the fits. To provide rigorous error estimates it is necessary to allow for arbitrarily many additional parameters within the dispersive bounds (8) and (9). For "global" quantities like $|V_{ub}|$ it is possible to show by imposing only the very loose bounds $\sum_k |\rho_k| < 10$ in (2), or $\sum_k a_k^2 < 1$ in (5) that the extracted values are actually insensitive to the addition of more parameters. With a single lattice input value $F_+(16\ \mathrm{GeV}^2) = 0.8 \pm 0.1$, we find

$$|V_{ub}| = 3.7 \pm 0.2\,^{+0.6}_{-0.4} \pm 0.1 = (3.7 \pm 0.2) \times \frac{0.8}{F_+(16\ \mathrm{GeV}^2)},$$
$$F_+(0) = 0.25 \pm 0.04 \pm 0.03 \pm 0.01 = (0.25 \pm 0.04) \times \frac{F_+(16\ \mathrm{GeV}^2)}{0.8}. \quad (12)$$

The first error is experimental, the second is theoretical from the lattice input, and the third is due to the uncertainty in the form-factor shape. For definiteness, the central values in (12) are obtained using the parameterization (5) with $\sum_k a_k^2 < 0.01$, and the third error is very conservatively estimated by adding the maximum variation of the boundaries of the 1σ interval induced by relaxing the bound to $\sum_k a_k^2 < 1$.

For less global quantities, like the slope of the form factor at $q^2 = 0$, the very loose bounds (8) and (9) are not sufficient to tightly constrain the impact of arbitrarily many additional parameters. In this case we adopt more realistic estimates for the bounds, and find

$$10^3\left|V_{ub}F_+(0)\right| = 0.92 \pm 0.11 \pm 0.03,$$
$$\left(m_B^2 - m_\pi^2\right)\frac{F'_+(0)}{F_+(0)} = 1.5 \pm 0.6 \pm 0.4,$$
$$(1-\alpha)^{-1} = 8^{+2}_{-7} \pm 7. \quad (13)$$

The first error is experimental, and the second is due to uncertainty in the form-factor shape (these quantities are independent of the form-factor normalization). The central values in (13) are again obtained using the parameterization (5) with $\sum_k a_k^2 < 0.01$, and the shape error is conservatively estimated by adding the maximum variation of the boundaries of the 1σ interval when the bound is relaxed to $\sum_k a_k^2 < 0.1$.

While the conventional dispersive bound approach provides an elegant means of demonstrating formal convergence properties with the minimal assumption of form-factor analyticity and the convergence of an operator product expansion, some caution is required in order to avoid misinterpreting the results. Firstly, for certain observables, e.g., $|V_{ub}|$, the fits are much more tightly constrained by the data than by the unitarity-based dispersive bound. This leads to the happy conclusion that the errors on $|V_{ub}|$ do not depend on the chosen parameterization or the exact value of the bound, and the analysis lends itself to a

straightforward statistical interpretation. Secondly, other important observables, such as the slope of the form factor, *are* sensitive to the addition of more parameters than can be constrained by the data, but are allowed by the unitarity bound. Since this bound is overestimated, presumably by orders of magnitude, a reliance on this procedure would lead to the pessimistic conclusion that almost no information at all can be extracted from the data for these quantities. In such cases, we propose to use tighter bounds, which follow from the scaling behavior of the bounded quantity in the heavy quark limit.

Apart from establishing order-of-magnitude estimates for the bounds in (8) and (9) by heavy-quark power counting, none of the above analysis relies on heavy-quark, large-recoil or chiral expansions, or on the associated heavy-quark, soft-collinear or chiral effective field theories. However, the semileptonic data can be used to test predictions from these effective field theories, and to determine low-energy parameters that can be used as inputs to the calculation of other processes. For example, using the experimental result $\mathrm{Br}(B^- \to \pi^- \pi^0) = (5.5 \pm 0.6) \times 10^{-6}$ [17] together with $|V_{ub}| F_+(0)$ from (13), we find

$$\frac{\Gamma(B^- \to \pi^- \pi^0)}{d\Gamma(\bar{B}^0 \to \pi^+ \ell^- \bar{\nu})/dq^2|_{q^2=0}} = 0.76^{+0.22}_{-0.18} \pm 0.05 \ \mathrm{GeV}^2, \quad (14)$$

where the first error is experimental, and the second is due to the form-factor shape uncertainty in (13). Such ratios provide a strong test of factorization [18]. The leading-order prediction for this ratio, corresponding to the "naive" factorization picture where hard-scattering corrections are neglected, yields $16\pi^2 f_\pi^2 |V_{ud}|^2 (C_1 + C_2)^2/3 = 0.62 \pm 0.07 \ \mathrm{GeV}^2$. This uncertainty includes only the effects of varying the renormalization scale of the leading-order weak-interaction coefficients [19] between $m_b/2$ and $2m_b$. This may be compared to the prediction of Beneke and Neubert [20] who use QCD factorization theorems for two-body decays to work beyond leading order and include the effects of hard-scattering terms, obtaining for the same ratio, $0.66^{+0.13}_{-0.08} \ \mathrm{GeV}^2$. The uncertainty in their prediction is dominated by the uncertainty in the light-cone distribution amplitudes (LCDAs) of the B- and π-mesons. Bauer et al. [13,21] evaluate the same factorization theorems using a different strategy: they use experimental results for other $B \to \pi\pi$ decays to determine the part involving the LCDAs from data, which is possible if all power corrections, and perturbative corrections of order $\alpha_s(m_b)$, are neglected. For the ratio (14) they find $1.27^{+0.22}_{-0.29} \ \mathrm{GeV}^2$, where we display only experimental errors. The semileptonic data provides important information on otherwise poorly constrained hadronic parameters entering these processes.

As a second application, the parameter δ measuring the relative size of hard-scattering and soft-overlap contributions in the $B \to \pi$ form factor can be related to the slope of the form factor at $q^2 = 0$ [12]. Extrapolated to zero recoil, the lattice calculations in [5,6] give for the slope of the F_0 form factor, $\beta \equiv [(m_B^2 - m_\pi)^2 F_0'(0)/F_+(0)]^{-1} = 1.2 \pm 0.1$. Together with (13) this yields

$$\delta \equiv 1 - \frac{m_B^2 - m_\pi^2}{F_+(0)} \left(\left.\frac{dF_+}{dq^2}\right|_{q^2=0} - \left.\frac{dF_0}{dq^2}\right|_{q^2=0} \right)$$
$$= 0.4 \pm 0.6 \pm 0.1 \pm 0.4, \quad (15)$$

where the first error is experimental, the second is theoretical from the lattice determination of β, and the third is due to the form-factor shape uncertainty in (13). Establishing the relative size of the hard-scattering and soft-overlap contributions from the semileptonic data provides another important input to factorization analyses of hadronic B decays. The above result for δ does not unambiguously establish $\delta \neq 0$ which signals the presence of hard-scattering terms, but it disfavors the opposite scenario, $\delta \approx 2$, where the form factor is completely dominated by hard-scattering. More data will help reduce both the experimental and shape-uncertainty errors for this quantity.

As a third application, the form factor $F_+(0)$ and shape observable α determine the coupling constant $g_{B^* B\pi}$ via

$$\frac{f_{B^*} g_{B^* B\pi}}{2m_{B^*}} \equiv \frac{F_+(0)}{1-\alpha} = 2.0^{+0.6}_{-1.6} \pm 0.2 \pm 1.7, \quad (16)$$

where the first error is experimental, the second is theoretical from the lattice form-factor normalization, and the final error is due to the form-factor shape uncertainty, determined as in (13). Since the semileptonic data is concentrated at small q^2, it is not very sensitive to the detailed structure of the sub-threshold pole and dispersive integral in (1). In fact, the data do not yet definitively resolve a distinct contribution of the B^* pole, although the opposite scenario—dominance by the B^* pole in (1)—is ruled out [12].

Our implementation of the bounds in (8) and (9) could be formalized in terms of standard methods of constrained curve fitting [22]. In this language, we have enforced a "prior" probability function which is constant if the parameters obey the bound on $\sum_k |\rho_k|$ or $\sum_k a_k^2$, and zero otherwise. For simplicity, we then performed a χ^2 fit, assuming sufficient statistics that the data is Gaussian distributed. The resulting error estimates should be conservative. Firstly, this prior allows equal probability for parameter values that are near the bound, even though we believe such values are increasingly unlikely. Other prior functions may be considered—for example, in the case of the series parameterization (5), a Gaussian prior on the variable $(-\log_{10} \sum_k a_k^2)$, with mean and standard deviation of order unity. Secondly, in estimating errors based on $\Delta\chi^2$, we neglect the fact that bounds enforce restrictions that renormalize the probability distributions, and to the extent that the bounds are relevant, this tends to overestimate errors. As a simple example, if an absolute bound happened to coincide with the boundary of the "1σ" interval obtained for an observable based on $\Delta\chi^2 = 1$, we would estimate that the observable was within the interval with only $\sim 68\%$ confidence, whereas the bounds guarantee this with 100% confidence. In a more refined analysis, a direct evaluation of the statistical integrals could account for such boundary effects. An alternative procedure employed in [9], and generalized in [23] to include shape information from experiment, has a slightly more complicated statistical interpretation. Here theory information on the form factor, combined with the dispersive bounds, is used to generate a statistical sample of "envelopes", each consisting of the curves defined at each q^2-point by the minimum and maximum values that the form

factor can take. (Note that some curves may be ruled out by the bounds, yet allowed by the envelopes, which are generated by extremizing point-by-point in q^2.) This sample of envelopes is then combined with experimental branching fractions to determine a distribution for $|V_{ub}|$ or other observables. Working in terms of parameters a_k allows the experimental and lattice data to be treated on the same footing, and yields a more straightforward interpretation of the constraints enforced by the bounds. Fortunately, these complications play an extremely minor role in the case of $|V_{ub}|$. As illustrated by Fig. 1, the errors are very nearly Gaussian, and nearly identical results are obtained using different parameterizations, and widely different values for the bounds. A more refined statistical analysis might be useful for those shape observables that show sensitivity to the bounds, to extract as much information as possible from the experimental data.

In summary, we have shown that the form-factor shape information necessary for a precise extraction of $|V_{ub}|$ is now entirely determined from experiment. Rather than relying on theoretical models for this shape, the current and future experimental data can instead be used as a precision tool for testing theory predictions and determining hadronic parameters in other processes. For example, the ratio in (14) should be predicted with good accuracy from the factorization approach to hadronic B decays, and can be even more firmly established once the hard-scattering contribution in (15) is determined more precisely from data. The methodology employed here for in B decays can be validated in the analogous situation of semileptonic D decays, where experiment and lattice cover the entire range of q^2. Note that we only used lattice input for the form factor at a single q^2-value, to avoid theoretical biases on the form-factor shape, and to emphasize the conclusion that the shape is determined by experiment; however, studying the form-factor shape provides an important test of lattice calculations. Our results show that with improved lattice data, an exclusive measurement of $|V_{ub}|$ that rivals or even surpasses the inclusive determination is possible.

Acknowledgements

We thank A. Kronfeld, H. Quinn and I. Stewart for discussions. We are grateful to the Institute for Nuclear Theory (Seattle, WA) for hospitality where a part of this work was completed. Research supported by the Department of Energy under Grants DE-AC02-76SF00515 and DE-AC02-76CH03000. Fermilab is operated by Universities Research Association Inc., under contract with the US Department of Energy.

References

[1] CLEO Collaboration, S.B. Athar, et al., Phys. Rev. D 68 (2003) 072003, hep-ex/0304019.
[2] Belle Collaboration, K. Abe, et al., hep-ex/0408145.
[3] BaBar Collaboration, B. Aubert, hep-ex/0507003.
[4] BaBar Collaboration, B. Aubert, hep-ex/0506064.
[5] M. Okamoto, et al., Nucl. Phys. B (Proc. Suppl.) 140 (2005) 461, hep-lat/0409116.
[6] J. Shigemitsu, et al., Nucl. Phys. B (Proc. Suppl.) 140 (2005) 464, hep-lat/0408019.
[7] C. Bourrely, B. Machet, E. de Rafael, Nucl. Phys. B 189 (1981) 157.
[8] C.G. Boyd, B. Grinstein, R.F. Lebed, Phys. Rev. Lett. 74 (1995) 4603, hep-ph/9412324.
[9] L. Lellouch, Nucl. Phys. B 479 (1996) 353, hep-ph/9509358.
[10] C.G. Boyd, M.J. Savage, Phys. Rev. D 56 (1997) 303, hep-ph/9702300.
[11] D. Becirevic, A.B. Kaidalov, Phys. Lett. B 478 (2000) 417, hep-ph/9904490.
[12] R.J. Hill, hep-ph/0505129, Phys. Rev. D, in press.
[13] M.C. Arnesen, B. Grinstein, I.Z. Rothstein, I.W. Stewart, Phys. Rev. Lett. 95 (2005) 071802, hep-ph/0504209.
[14] C.G. Boyd, B. Grinstein, R.F. Lebed, Nucl. Phys. B 461 (1996) 493, hep-ph/9508211.
[15] I. Caprini, L. Lellouch, M. Neubert, Nucl. Phys. B 530 (1998) 153, hep-ph/9712417.
[16] P. Ball, R. Zwicky, Phys. Lett. B 625 (2005) 225, hep-ph/0507076.
[17] HFAG, http://www.slac.stanford.edu/xorg/hfag/;
BaBar Collaboration, B. Aubert, et al., Phys. Rev. Lett. 94 (2005) 181802, hep-ex/0412037;
Belle Collaboration, Y. Chao, et al., Phys. Rev. D 69 (2004) 111102, hep-ex/0311061;
CLEO Collaboration, A. Bornheim, et al., Phys. Rev. D 68 (2003) 052002, hep-ex/0302026.
[18] M. Bauer, B. Stech, M. Wirbel, Z. Phys. C 34 (1987) 103;
J.D. Bjorken, Nucl. Phys. B (Proc. Suppl.) 11 (1989) 325.
[19] G. Buchalla, A.J. Buras, M.E. Lautenbacher, Rev. Mod. Phys. 68 (1996) 1125, hep-ph/9512380.
[20] M. Beneke, M. Neubert, Nucl. Phys. B 675 (2003) 333, hep-ph/0308039.
[21] C.W. Bauer, D. Pirjol, I.Z. Rothstein, I.W. Stewart, Phys. Rev. D 70 (2004) 054015, hep-ph/0401188.
[22] For an introduction, see G.P. Lepage, B. Clark, C.T.H. Davies, K. Hornbostel, P.B. Mackenzie, C. Morningstar, H. Trottier, Nucl. Phys. B (Proc. Suppl.) 106 (2002) 12, hep-lat/0110175.
[23] M. Fukunaga, T. Onogi, Phys. Rev. D 71 (2005) 034506, hep-lat/0408037.